

Effect of deposition time on the structural, optical and electrical properties of CuAlS₂ thin films prepared by chemical bath deposition technique

B. Y. Taher^{a,*}, A. S. Ahmed^b

^aCollege of Agriculture, University of Anbar, Iraq

^bDepartment of Physics, College of Science, University of Baghdad, Iraq

CuAlS₂ thin films have been prepared on glass substrates by Chemical bath deposition (CBD) technique at a substrate temperature (T_s) 75°C, pH value 10.5. The Effect of three different deposition times (20, 30, and 40 minute) on the structural, optical and electrical properties of deposit thin films was studied. The X-ray diffraction (XRD) patterns showed that the films have an amorphous structure with simple enhancement in the structure of the films with the higher deposition time. Field emission scanning electron microscopy (FESEM) analysis of thin films showed that the deposited films were a good surface morphology, homogenous and uniform spherical nanoparticles over the substrate surface with very little agglomerated particles. Atomic force microscopy (AFM) showed the topography of deposited films has nanoparticles with structures like conical and spherical shape with the average grain sizes increase with increasing deposition time. The optical analysis by UV-Vis Spectrophotometer showed high absorption in the ultraviolet region, with absorption edge and direct energy gaps (3.95 to 3.60 eV) decreases with increasing the deposition time. The electrical results from Hall effect measurements showed that the values of resistivity, conductivity, mobility, and carrier concentration were varied in range (0.31 to 0.52 ohm.cm), (1.83 to 3.23(ohm.cm)⁻¹), (5.01×10² to 2.17×10³ cm²/V.S), and (5.26×10¹⁵ to 2.39×10¹⁶ cm⁻³), respectively. Also, n and p conductivity were investigated of prepared films depending on the deposition time.

(Received June 6, 2021; Accepted September 7, 2021)

Keywords: CuAlS₂ thin films, Optical properties, Electrical properties, Chemical bath deposition technique, Structural properties, Morphological, Effect of deposition time

1. Introduction

Ternary chalcopyrite semiconductors have attracted much attention of the scientists. CuAlS₂ compound among them is an inexpensive and promising material due to their many technological applications, such as optoelectronics, photovoltaic, solar cells, detectors, thin films field, light emitting diodes, and a wide direct energy gap which can be suitable to use as a transparent back contact in solar cells [1,2,3,4].

There are many techniques used to prepare ternary CuAlS₂ thin films, such as powder metallurgy technique [5], chemical spray pyrolysis [6, 7], atomic layer deposition [8], metal organic chemical vapour deposition (MOCVD) [9], Electrophoretic Deposition (EPD) [10], Electron beam evaporation [11], hydrothermal method (HT) [12], vacuum thermal evaporation [13], chemical vapour transport (CVT) technique [14], wet chemical method [15,16], direct polyol methods [17,18], simple colloidal route [19], spark plasma sintering [20], sulfurization of metallic precursors in a vacuum [21], and chemical bath deposition technique (CBD) which were used by many researchers.

Tariq J. et al., prepared CuAlS₂ thin films by CBD technique on glass substrates, from aqueous solutions with Triethanolamine (TEA) as a complex agent, where all films were amorphous structure. Optical properties showed direct energy gap 2.81 and 2.4 eV as deposited and annealing, respectively [22]. S.M. Ahmad prepared CuAlS₂ thin films by SPS and CBD technique from aqueous solutions with Triethanolamine (TEA) a complex agent, with deposition

* Corresponding author: ag.bilal.yaseen@uoanbar.edu.iq

time 48h at room temperature. Prepared films by the CPS has a polycrystalline while amorphous structure for CBD, optical properties showed a direct energy gap with 3.00 eV by CPS and 2.8 eV by CBD technique [23]. Sunil H. Chaka et al. prepared CuAlS₂ thin films by dip coating deposition from aqueous solutions with Triethanolamine (TEA) as a complex agent, and with pH 9.5. Optical studies showed a direct energy gap 3.82 eV [24].

There are many advantages to use CBD technique comparing with other techniques such as low cost, available and inexpensive, environmentally friendly, deposition temperature is low and safe to use, simply controlling with deposition parameters, deposition with large area of thin films, chemical precursors are available and dissolved in distilled water, nontoxic for using, and simplicity for the preparation of films on various substrates. [25]

To our knowledge, up to now, only a few works have been done with using disodium salt dehydrate Na₂EDTA.2H₂O as the complex agent to deposited CuAlS₂ thin films by CBD technique.

In this study CuAlS₂ thin films were deposited at T_s 75°C in alkaline medium with pH 10.5, using an aqueous solution of copper (II) sulfate pentahydrate (CuSO₄.5H₂O), aluminum sulphate [Al₂(SO₄)₃.16H₂O], thiourea [(NH₂)₂CS], ammonia solution (NH₃), with 0.04M of EDTA disodium salt dehydrate Na₂EDTA.2H₂O as the complex agent. Effect of different deposition times (20, 30, and 40 min.) was studied. The aim of this study to find the best prepared conditions for getting the high quality of deposited thin films, and using it in different optoelectronic devices.

2. Experimental details

Solution of CuAlS₂ was prepared with molar concentrations of precursors (0.05, 0.025, 0.1M) from copper (II) sulfate pentahydrate [CuSO₄.5H₂O] (Honeywell Fluka, Germany), Aluminum sulphate [Al₂(SO₄)₃.16H₂O] (Thomas Baker, India), and Thiourea [(NH₂)₂CS] (Merck, Germany), which used as a sources of Cu, Al, and S ions, respectively. EDTA disodium salt dihydrate [Na₂EDTA.2H₂O] (Glenthams, UK) with 0.03M was used as a complex agent in all prepared solutions. Effect of different deposition times (20, 30, and 40 min.) was studied.

Before the solutions were mixed, the glass substrates were cleaned by the following procedure, in the first the glass substrates were cleaned by distilled water and shampoo, followed by distilled water only at 100°C on hotplate, and dried in air before immersed in nitric acid for 48 h, after that washed by distilled water before its immersed in HCl for 24 h, and after cleaned by distilled water before its immersed in ethanol, followed in acetone for 30 min., and finally washed by distilled water and lifted to dry in air. The advantage of cleaned procedure to enhanced the nucleation and adherent thin films on glass substrates.

The solution was performed for concentrations of precursors (0.05, 0.025, 0.1)M, by mixing 10ml of copper sulfate CuSO₄.5H₂O (0.05M) added into beaker 100 ml, and stirred on hotplate heater at 40°C by magnetic dipole for five min., and this process was repeated continuously for all prepared solution, added to it 10ml of Na₂EDTA (0.03M), and stirred for 5 min., 5 ml of Al₂(SO₄)₃.16H₂O (0.05M) added to solution and stirred for 5 min., after that ammonia solution added to solution to adjust pH value to 10.5, and finally 10 ml of (NH₂)₂CS (0.1M) added slowly to solution, after that, the magnetic dipole was left from the beaker, and two glass substrate face to face was immersed vertically in beaker after cleaned procedure, and the beaker was putted directly in water bath which was adjusted at temperature 75±0.2 °C. The deposition time was calculated at the time of lifting the beaker from the water bath, and the substrates were carried out from the beaker, and were washed by distilled water and lifted to dry in air.

Fig.1 show the following changes were observed after the beaker was kept in a water bath, where, when ammonia solution were added to the solution, The color of the solution in the first two min., changed from light sky to light blue, after two min., changed to bold blue. While, when the thiourea was added after that the solution, the color changed to light green after two min., and to a deep yellowish after one min., and after three min., the solution gradually changed to bold orange or brown color [26], and finally after two min., the solution became black color[18].

Color changing for the solution in different interval times affected mainly by deposition parameters such as deposition time, which effect on reaction rate through deposition process, and some of these observations of color changing were reported.[27,22,23,8].

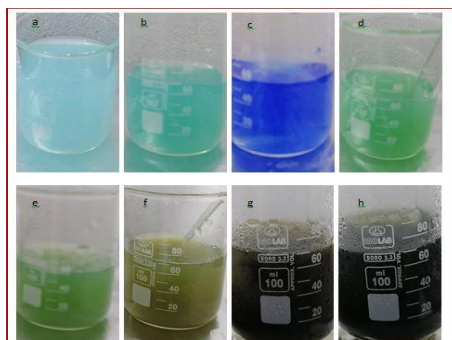


Fig. 1. (a, b, c, d, e, f, g and h) represent the main states of color changing respectively of deposit CuAlS₂ thin films.

The XRD patterns of deposit CuAlS₂ thin films were taken by the Phillips X-pert High Score PANalytical X-ray diffractometer with CuK α ($\lambda = 1.5406 \text{ \AA}$) radiation as a source, with the range of 2θ degree from 10.35° to 80.00° , with a step size (2θ) 0.05° , and scan step time 1s.

Optical measurements of deposit films were obtained by using a UV-Vis spectrophotometer model Cary 60 Agilent, with a wavelength range of 190-1200 nm at room temperature. Electrical measurements of deposit films were done at room temperature by using Hall Effect measurements, model IRASOL/HSR-24 AC Hall Effect. The Surface morphology and cross section of deposit films were tested by field emission scanning electron microscopy (FESEM) model)ZEISS Supra 35 VP) with high resolution mode, and with magnification 100 KX. Topography of thin films were tested by atomic force microscopy (AFM), model JPK Nanowizard, Germany, where the physical size of surface topography of films are observed approximately from (2500, 2500) to (5000, 5000) nm.

3. Results and discussion

3.1. X-ray diffraction analysis

The X-ray diffraction patterns of deposit CuAlS₂ thin films onto the amorphous glass substrate for deposition times 20, 30, and 40 min., are shown in Fig.2. The amorphous structure of all prepared thin films was observed, where no peaks in all films. This behavior has been mentioned by other researchers [22,23]. The amorphous nature of deposited films may be due to the low thickness, nanoparticles, which have a small grain size, and the amorphous of glass substrate, which cause weakness in the intensity of X-ray diffraction patterns [28].

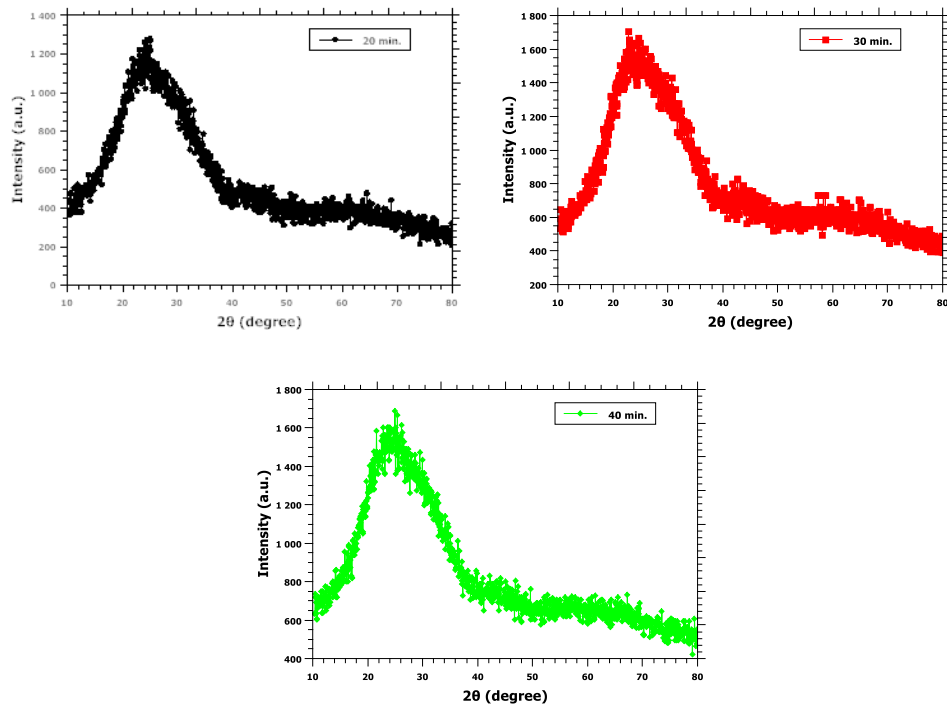


Fig. 2. XRD patterns for CuAlS_2 thin films at deposition time a) 20, b) 30, and c) 40 min.

3.2. Thickness measurements

The average thickness of CuAlS_2 thin films was done by cross section analysis of deposit films which are shown in Fig.3. The values of thickness average were 450, 110, and 200 nm for deposition time 20, 30, and 40 min., respectively. The thickness decreases with deposition time from 20 to 30 min., and then rises at 40 min. Therefore, the thicknesses of deposit films were affected by the deposition time, where the thickness was not exceeded by increasing the deposition time may be the solution of prepared films arrived to saturation state, and this means the homogenous processes on deposit layer of films were reduced with increasing the deposition time.

The values of thickness average were used to calculate the parameters of optical properties of deposit thin films.

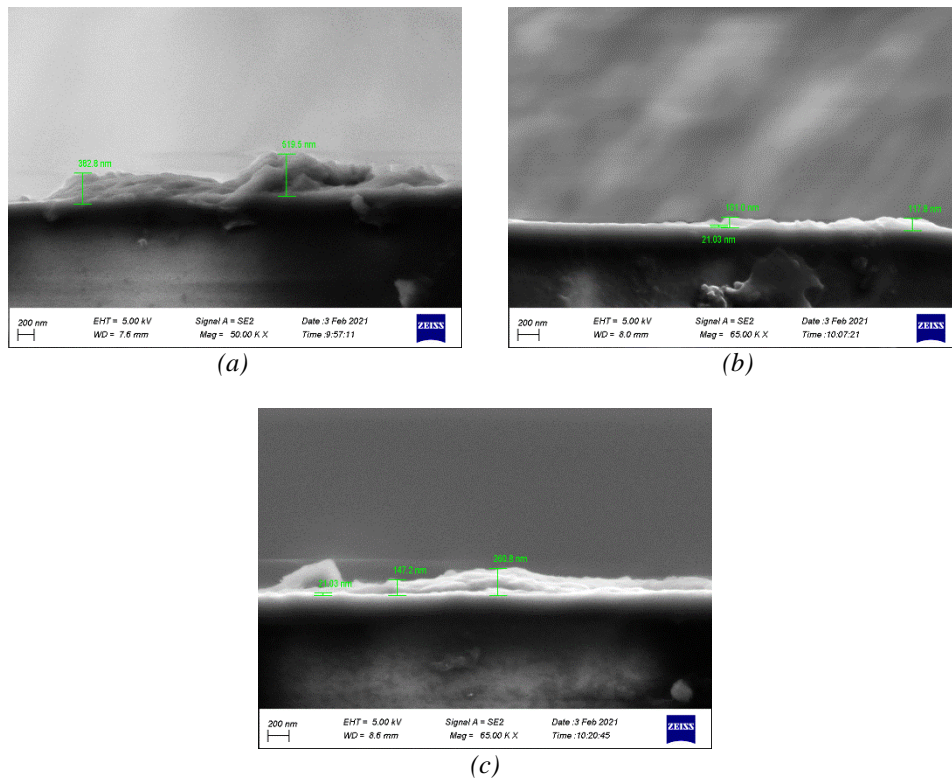


Fig.3. Cross section images of CuAlS_2 thin films for deposition times (a) 20, (b) 30, and (c) 40 min.

3.3. Optical properties measurements

Fig.4 shows the UV-Vis absorption spectra of CuAlS_2 thin films with various deposition times in the wavelength range of 200 to 1100 nm.

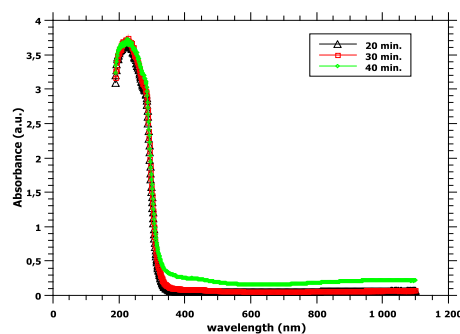


Fig. 4. Absorbance spectrum of CuAlS_2 thin films for deposition times (a) 20, (b) 30, and (c) 40 min.

The spectrum shows high absorption in the ultraviolet region with an absorption edge at 214 to 237 nm. The absorption edge decreases with increasing the deposition time from 20, 30, and 40 min., respectively.

A sharper absorber edge means fewer impurities and defects in the deposited films, [29].

Fig. shows the direct energy gap was calculated by plotting $(ahv)^2$ as a function of photon energy ($h\nu$) of the films. The optical energy gap values are obtained by extrapolating the linear portion of the plots to intercept the photon energy axis [30]. The variation of energy gaps with deposition times is tabulated in Table 1.

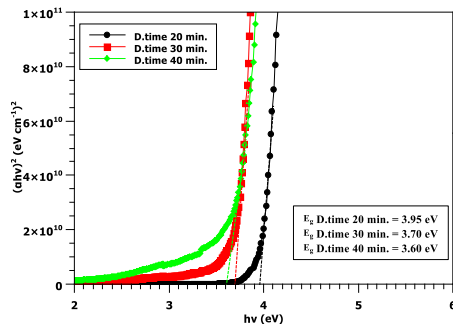


Fig. 5. Energy gap of CuAlS_2 thin films for deposition times (a) 20, (b) 30, and (c) 40 min.

Table 1. Values of direct energy gap for depositing CuAlS_2 thin films.

Deposition time	E_g (eV)
20	3.95
30	3.70
40	3.60

The direct band gap E_g values were found to vary between 3.52 to 3.95 eV depending on the deposition time. It is clear from Table 1 that energy band gap is affected by deposition time, where the energy gap decrease with increasing deposition time which are shown in Fig.6. The variation in the energy values may be variation in grain size, which are observed from FESEM and AFM results, where the energy gap decrease with the increasing grain size due to size effect [29]. The energy gap values for CuAlS_2 thin films which were prepared in this work are greater than with that found by Alwan et al ($E_g = 2.81$ eV) [22], Ahmad ($E_g = 3.00$ eV) [23], Naveena and Chadra ($E_g = 3.26$ eV) [31], and the value of energy gap at deposition time 40 min., slightly agreement with Bhandari et al ($E_g = 3.5$ eV) [21].

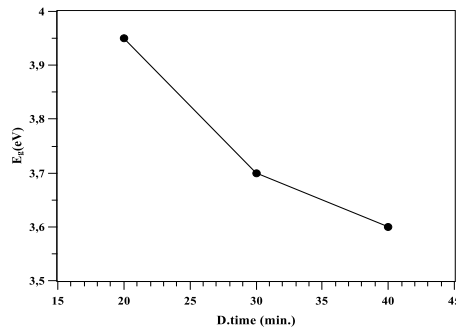


Fig. 6. Energy gap of CuAlS_2 thin films as a function for different deposition times 20, 30, and 40 min.

Fig.7 shows the transmittance (T%) and the reflectance (R%) spectra as a function of wavelength from 200 to 1200 nm for CuAlS_2 thin films at different deposition times 20, 30, and 40 min. The transmittance decreases with increasing the deposition time, where the maximum transmittance is observed at wavelength 700 nm for all deposition times. Transmittance reaches 90% for deposition times 20 and 30 min., but it decreases to 70% for deposition time 40 min., due to the increasing of absorbance as a result of decreasing of the energy gap.

The transmittance increases at wavelengths from 200 to 700 nm gradually at deposition times 20 and 30 min., while it increases quickly at deposition time 40 min. In the wavelength range from 700 to 1200 nm, the transmittance becomes approximately constant at deposition time 20 and 30 min., while at deposition time 40 min., the transmittance decreases gradually; therefore

these materials can be used as a window layer in solar cell and infrared devices. The reflectance behavior of deposit films is reciprocal the transmittance.

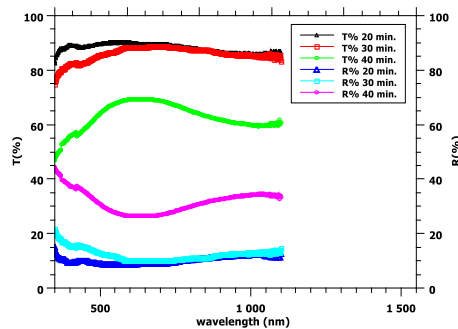


Fig. 7. Transmittance and Reflectance spectrum of CuAlS_2 thin films.

3.4. Electrical properties analysis

The electrical properties of CuAlS_2 thin films measured by Hall Effect measurement at room temperature. Table 2 shows the Hall parameters of deposit CuAlS_2 thin films of different deposition time (20, 30, and 40 min.). The conductivity (σ) of prepared films decreases with increasing the deposition time from 20 to 30 min., and after that it increases with increasing the deposition time from 30 to 40 min. The behavior of resistivity (ρ) inversely compares with that observed for conductivity which are shown in Fig.8 (a). Values of resistivity and conductivity were in the range (0.31 to 0.547 ohm.cm) and $(1.93$ to 3.23 $(\text{ohm.cm})^{-1}$), respectively which are a good agreement with that found by [11].

The charge carrier concentration (n) of prepared films decreases with increasing the deposition time from 20 to 30 min., and after that it increases with increasing the deposition time from 30 to 40 min., and this behavior is same as of that of the thickness of prepared films. This behavior due to the film with high thickness has more carrier concentration, and the verse versa. Values of carrier concentration were varied in the range $(5.26 \times 10^{15}$ to $2.39 \times 10^{16} \text{ cm}^{-3})$ which are a good agreement with that found by Chaki et al $(\sim 10^{16} \text{ cm}^{-3})$ [32].

The mobility of charge carriers (μ) for prepared films increases with increasing the deposition time from 20 to 30 min., and after that it decreases with increasing the deposition time from 30 to 40 min. The behavior of mobility inversely compared with that observed for carrier concentrations which are shown in Fig.8 (b).

The prepared films with low carrier concentration have high mobility, due to the movement of charge carriers are freer, and verse versa. Values of mobility were varied in the range $(501$ to 2170 $(\text{cm}^2\text{V}^{-1}\text{s}^{-1}))$ which are greater than found by Min et al $(1.1 \text{ cm}^2\text{V}^{-1}\text{s}^{-1})$ [20].

The type of conductivity of prepared films was n-type at deposition time 20 and 40 min., while was p-type at deposition time 30 min., both types of conductivity were found by [14,32].

Table 2. Hall parameters of as deposited CuAlS_2 thin films for different deposition times.

Sample	n (cm^{-3})	ρ (ohm.cm)	σ (ohm.cm) ⁻¹	μ ($\text{cm}^2\text{V}^{-1}\text{s}^{-1}$)	Type of conductivity
CuAlS_2 at 20 min.	2.39×10^{16}	0.521	1.92	501	n
CuAlS_2 at 30 min.	5.26×10^{15}	0.547	1.83	2170	p
CuAlS_2 at 40 min.	1.32×10^{16}	0.310	3.23	1530	n

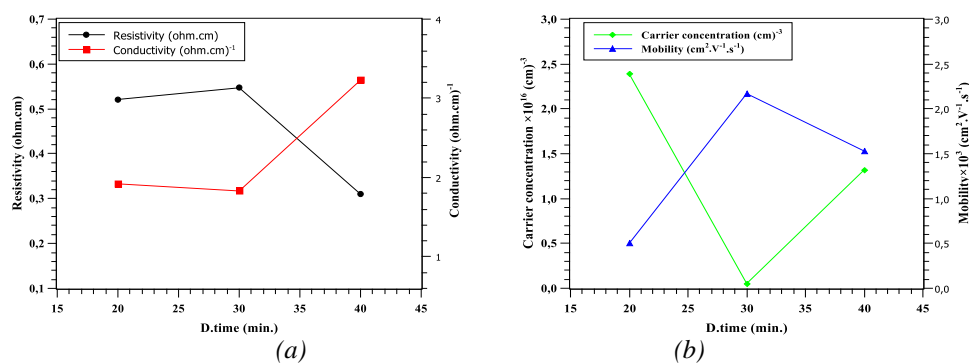


Fig. 8. (a) Resistivity and conductivity, (b) carrier concentration and mobility of CuAlS₂ thin films as a function of deposition time 20, 30, and 40 min.

3.5. Surface morphological analysis

3.5.1. FESEM characterization

Morphological properties of CuAlS₂ thin films were done by field emission scanning electron microscopy (FESEM). FESEM images of prepared films at deposition times (20, 30, and 40 min.) were shown in Fig.9. The prepared film at 20 min., show homogenous and uniform spherical nanoparticles with a good surface morphology over the substrate surface and some agglomerated particles were observed. The average grain size was about 19 nm. At deposition time 30 min., the prepared film shows spherical nanoparticles with an average grain size about 47 nm, and some agglomerated particles like nanotube shape were observed, which are attached together with the diameter about 80 nm and length about 1.8 μm. The prepared film at deposition time 40 min., shows spherical nanoparticles covering large areas of total film with an average grain size about 51 nm, and very little agglomerated particles were found. The morphological properties at deposition time 40 min., showed enhancement in the microstructure of prepared film. The grain sizes of deposit films increase with the increasing the deposition time are shown in Table 2, and this may due to the increasing the growth process in the films.

The values of G.S in this work are smaller than with that found (380 nm and 150 nm) by Ahmad [23], and agreement with that found (19.09 nm) by Moataz et al [5].

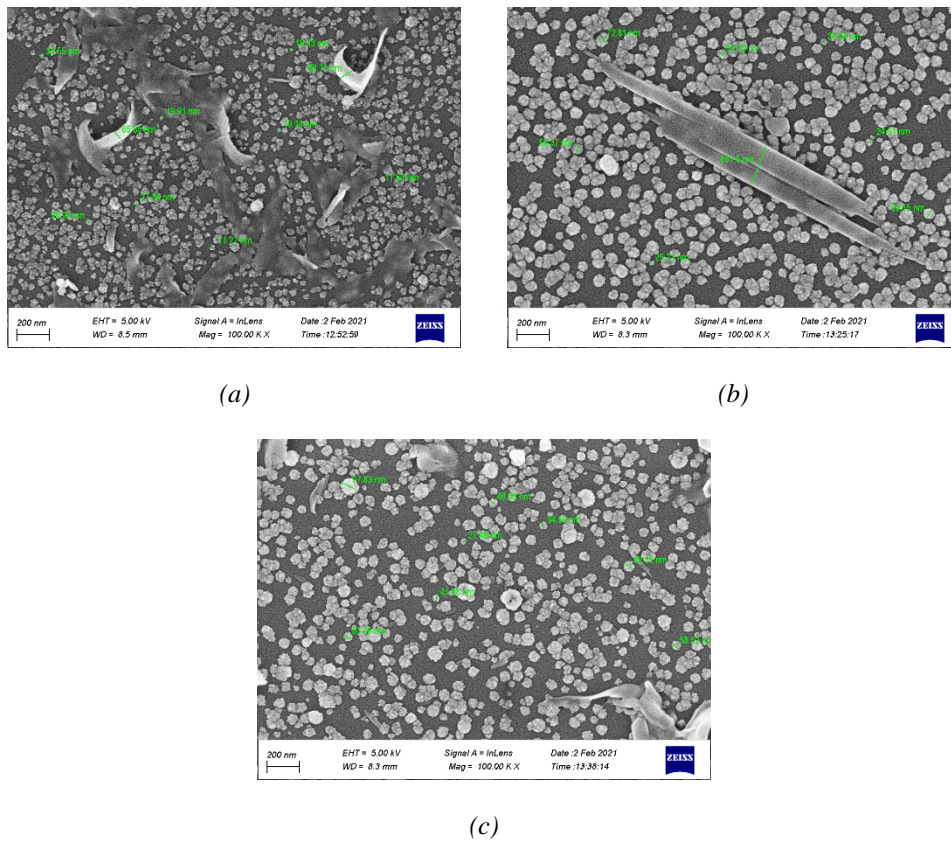


Fig. 9. FESEM images of prepared CuAlS_2 thin films for deposition times (a) 20, (b) 30, and (c) 40 min.

3.5.2. AFM characterization

Topography properties of prepared CuAlS_2 thin films were taken by atomic force microscopy (AFM). AFM images for prepared CuAlS_2 thin films on glass substrate at deposition time 20, 30, and 40 min., were shown in Fig.10. Values of average grain size (G.S), surface roughness, and root mean square (rms) roughness for prepared films were tabulated in Table 3.

Prepared film at 20 min. was smooth, good adhesion to the substrate, and homogeneous distribution on the substrate surface, also the film showed structures like conical and spherical shape without any distances between them and covering all regions of the total film. While for prepared films at 30 and 40 min., have the same structures as conical and spherical shapes, but at deposition time 30 min., the distances between grains were less than at deposition time 40 min. The increasing in the deposition time leads to increase the nanoparticles to the large crystals due to the increasing the growth process [33].

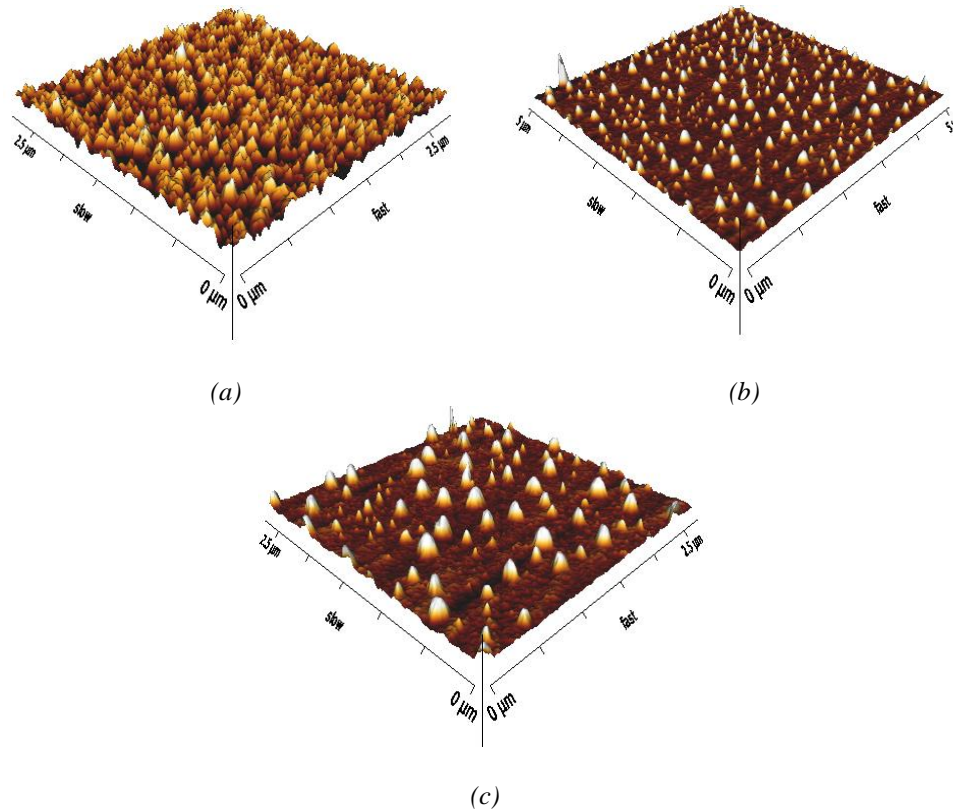


Fig.10. AFM images of prepared CuAlS_2 thin films for deposition times (a) 20, (b) 30, and (c) 40 min.

Table 2, shows values of the average grain size (G.S) increases in the range (100 to 156 nm), whereas root mean square (rms) roughness decreases in the range (4.35 to 1.54 nm) with the increasing the deposition time (20 to 40 min.). But the surface roughness decrease from 3.5 to 0.87 nm for the deposition time from 20 to 30 min., and increase slightly to 0.90 nm at 40 min.

Table 3. Values of (G.S from FESEM and AFM, surface roughness, rms roughness) of deposit CuAlS_2 thin film at different deposition times).

D.time(min.)	Average G.S (nm) by FESEM	by AFM measurements		
		Average G.S (nm)	surface roughness (nm)	rms roughness(nm)
20 min.	19	100	3.5	4.35
30 min.	47	147	0.87	1.67
40 min.	51	156	0.90	1.54

The same manner was observed for average grain sizes which were found by FESEM and AFM results which are shown in the Table 3, and the difference values of G.S due to the different characterization between FESEM which analyzes morphological properties, and AFM which analyzes topography of films. This means the deposition time plays an important role to determine average grain sizes for prepared thin films.

4. Conclusions

In this study, CuAlS₂ thin films on amorphous glass substrates were prepared by using the CBD technique at substrate temperature 75°C and pH value 10.5, with different deposition times (20, 30, and 40 min.). The highlight above results is following:

The prepared films showed the amorphous structure. Increasing the deposition time gives simple enhancement in structure of prepared films, and this clear in the thin CuAlS₂ film at deposition time 30 and 40 min. The average thickness of deposit films decreases with deposition time from 20 to 30 min., and after that increases at 40 min., slightly.

The deposited films were a good surface morphology, homogenous and uniform spherical nanoparticles over the substrate surface with very little agglomerated particles. While the topography of deposited films showed nanoparticles with structures like conical and spherical shape. In general, the average grain sizes of thin films increase with increasing the deposition time.

The prepared films showed direct band gaps which were decreased from 3.95 to 3.6 eV with increasing deposition time, due to the increasing in grain size of thin films. The absorption spectrum shows high absorption in the ultraviolet region, and absorption edge decreases with increasing the deposition time.

At deposition time 30 min., the prepared films exhibit the minimum value for carrier concentration and conductivity, while the maximum value for resistivity and mobility. The type of conductivity of prepared films was n-type at deposition time 20 and 40 min., while was p-type at deposition time 30 min.

The obtained results of the prepared CuAlS₂ thin films can be suitable in many optoelectronics applications.

References

- [1] R. Brini, G. Schmerber, M. Kanzari, J. Werckmann, B. Rezig, *Thin Solid Films* **517**(7), 2191 (2009).
- [2] U. P. Verma, P. Jensen, M. Sharma, P. Singh, *Computational and Theoretical Chemistry* **975**(1-3), 122 (2011).
- [3] A. U. Moreh, M. Momoh, H. N. Yahya, B. Hamza, I. G. Saidu, S. Abdullahi, *International Journal of Physical and Mathematical Sciences* **8**(7), 1084 (2014).
- [4] A. N. Fioretti, M. Morales-Masis, *Journal of Photonics for Energy* **10**(04), 1 (2020).
- [5] M. H. Ata, E. Abdellateef, M. Elrouby, *Materials Science and Engineering B: Solid-State Materials for Advanced Technology* **261**(April), 114688 (2020).
- [6] S. M. Ahmad, *Optik*, (2016).
- [7] M. Caglar, S. Ilıcan, Y. Caglar, *Optics Communications* **281**(6), 1615 (2008).
- [8] N. Schneider, L. Duclaux, M. Bouttemy, C. Bugot, F. Donsanti, A. Etcheberry, N. Naghavi, *ACS Applied Energy Materials* **1**(12), 7220 (2018).
- [9] J. Damisa, B. Olofinjana, O. Ebomwonyi, F. Bakare, S. O. Azi, *Materials Research Express* **4**(8), (2017).
- [10] C. Guo, C. Yang, Y. Xie, P. Chen, M. Qin, R. Huang, F. Huang, *RSC Advances* **6**(47), 40806 (2016).
- [11] H. Kawaguchi, T. Ishigaki, T. Adachi, Y. Oshima, K. Ohmi, *Physica Status Solidi C Current Topics in Solid State Physics* **12**(6), 793 (2015).
- [12] S. Sukan, K. Baskar, R. Dhanasekaran, *Journal of Alloys and Compounds* **645**, 85 (2015).
- [13] M. Abaab, A. S. Bouazzi, B. Rezig, *Microelectronic Engineering* **51**, 343 (2000).
- [14] S. H. Chaki, K. S. Mahato, M. P. Deshpande, *Chinese Journal of Physics* **52**(5), (2014).
- [15] S. H. Chaki, K. S. Mahato, M. P. Deshpande, *Advanced Science Letters* **20**(5–6), (2014).
- [16] G. Harichandran, N. P. Lalla, *Materials Letters* **62**(8-9), (2008).
- [17] Y. Vahidshad, A. Irajizad, R. Ghasemzadeh, S. M. Mirkazemi, A. Masoud, *International Journal of Modern Physics B* **26**(31), (2012).
- [18] G. H. Yue, X. Wang, L. S. Wang, W. Wang, D. L. Peng, *Physics Letters, Section A: General*,

- Atomic and Solid State Physics **372**(38), 5995 (2008).
- [19] A. C. Poulouse, S. Veerananarayan, A. Aravind, Y. Nagaoka, Y. Yoshida, T. Maekawa, D. Sakthi Kumar, *Materials Express* **2**(2), 94 (2012).
- [20] M. L. Liu, Y. M. Wang, F. Q. Huang, L. D. Chen, W. D. Wang, *Scripta Materialia* **57**(12), 1133 (2007).
- [21] R. K. Bhandari, Y. Hashimoto, K. Ito, *Japanese Journal of Applied Physics, Part 1: Regular Papers and Short Notes and Review Papers* **43**(10), 6890 (2004).
- [22] T. J. Alwan, M. A. Jabbar, *Turkish Journal of Physics* **34**(2), 107 (2010).
- [23] S. M. Ahmad, *Applied Physics A: Materials Science and Processing*, (2017).
- [24] S. H. Chaki, K. S. Mahato, T. J. Malek, M. P. Deshpande, *Journal of Science: Advanced Materials and Devices* **2**(2), 215 (2017).
- [25] S. M. Ho, *Research Journal of Applied Sciences, Engineering and Technology* **11**(10), 1058 (2015).
- [26] B. Bhattacharyya, T. Pandit, G. P. Rajasekar, A. Pandey, *Journal of Physical Chemistry Letters* **9**(15), 4451 (2018).
- [27] K. A. Mohammed, S. M. Ahmed, R. Y. Mohammed, *Crystals* **10**(8), 1 (2020).
- [28] I. S. Najji, M. F. A. Alias, B. Y. Taher, A. A. J. Al-Douri, *Chalcogenide Letters* **15**(2), 83 (2018).
- [29] A. S. Najm, M. S. Chowdhury, F. T. Munna, P. Chelvanathan, V. Selvanathan, M. Aminuzzaman, K. Techato, N. Amin, M. Akhtaruzzaman, *Chalcogenide Letters* **17**(11), 537 (2020).
- [30] M. F. A. Alias, B. Y. Taher, I. S. Najji, S. Iqbal, A. Kayani, M. F. Mabrook, A. A. J. Al-Douri, *Chalcogenide Letters* **16**(12), 577 (2019).
- [31] D. Naveena, A. C. Bose, *AIP Conference Proceedings* **2115**(July), 1 (2019).
- [32] S. H. Chaki, K. S. Mahato, T. J. Malek, M. P. Deshpande, *Journal of Science: Advanced Materials and Devices*, (2017).
- [33] R. A. ismail, A. M. E. Al-Samarai, F. M. Ahmed, *Surfaces and Interfaces* **21**, 100753 (2020).